THE JOURNAL OF BIOLOGICAL CHEMISTRY
Vol. 278, No. 48, Issue of November 28, pp. 48404–48412, 2003

Printed in U.S.A.

Extracellular S100A1 Protein Inhibits Apoptosis in Ventricular Cardiomyocytes via Activation of the Extracellular Signal-regulated Protein Kinase 1/2 (ERK1/2)*

Received for publication, August 5, 2003, and in revised form, September 4, 2003
Published, JBC Papers in Press, September 6, 2003, DOI 10.1074/jbc.M308587200

Patrick Most‡§¶, Melanie Boerries§‖, Carmen Eicher‡, Christopher Schweda‡, Philipp Ehlermann‡, Sven T. Pleger‡, Eva Loeffler‡, Walter J. Koch‡‡, Hugo A. Katus‡, Cora-Ann Schoenenberger‖§§, and Andrew Remppis‡§§**

From ‡Innere Medizin III, Universität Heidelberg, 69115 Heidelberg, Germany, the ‖Maurice E. Müller-Institute, Biozentrum, University of Basel, 4056 Basel, Switzerland, and the ‡‡Department of Surgery, Duke University Medical Center, Durham, North Carolina 27710

S100A1 is a Ca^{2+}-binding protein of the EF-hand type that belongs to the S100 protein family. It is specifically expressed in the myocardium at high levels and is considered to be an important regulator of cardiac contractility. Because the S100A1 protein is released into the extracellular space during ischemic myocardial injury, we examined the cardioprotective potential of the extracellular S100A1 protein on ventricular cardiomyocytes *in vitro*. In this report we show that extracellularly added S100A1 protein is endocytosed into the endosomal compartment of neonatal ventricular cardiomyocytes via a Ca^{2+}-dependent clathrin-mediated process. S100A1 uptake protects neonatal ventricular cardiomyocytes from 2-deoxyglucose and oxidative stress-induced apoptosis *in vitro*. S100A1-mediated anti-apoptotic effects involve specific activation of the extracellular signal-regulated kinase 1/2 (ERK1/2) pro-survival pathway, including activation of phospholipase C, protein kinase C, mitogen-activated protein kinase kinase 1, and ERK1/2. In contrast, neither transsarcolemmal Ca^{2+} influx via the L-type channel nor protein kinase A activity seems to take part in the S100A1-mediated signaling pathway. In conclusion, this study provides evidence for the S100A1 protein serving as a novel cardioprotective factor *in vitro*. These findings warrant speculation that injury-dependent release of the S100A1 protein from cardiomyocytes may serve as an intrinsic mechanism to promote survival of the myocardium *in vivo*.

S100A1, a low molecular weight (M_r 10,000) Ca^{2+}-binding protein belongs to a multigenic family (21 members) of non-ubiquitous Ca^{2+}-modulated proteins to form an important subclass of EF-hand proteins. Importantly, S100 proteins exhibit cell- and tissue-specific expression and have been linked to Ca^{2+}-dependent regulation of a variety of S100 isoform-specific intracellular activities such as protein phosphorylation, enzyme activity, cell proliferation and differentiation, dynamics of cytoskeletal constituents, structural organization of membranes, intracellular Ca^{2+}-homeostasis, and inflammation (for reviews, see Refs. 1–3). S100A1 is the most abundant S100 protein isoform in striated muscle and has been identified as a novel positive inotropic intracellular regulator of cardiac as well as skeletal muscle Ca^{2+}-homeostasis and contractility (4–8).

However, growing evidence indicates that members of the S100 protein family also exert extracellular effects on their target cells (3). Although S100 proteins apparently lack the signaling sequences required for secretion, some S100 isoforms seem to follow secretory pathways that involve neither the classical endoplasmic reticulum/Golgi nor the alternative interleukin-1-like route (9). For instance, S100A8 and S100A9, expressed at high concentrations by myelomonocytic cells, are secreted by a novel tubulin-dependent pathway and then exert important roles in the regulation of inflammatory processes (9). Similarly, extracellular functions for S100B, which is secreted by astrocytes, have been described extensively (10). After secretion, S100B appears to exert both trophic and pro-survival effects on neurons via activation of the Ras/mitogen-activated protein (MAP)[1] kinase pathway (11, 12). Neurotrophic effects have also been reported for extracellular S100A4 and S100A12 protein based on the activation of the extracellular signal-regulated protein kinase (ERK1/2) signaling pathway (13, 14).

It has been shown that the S100A1 protein is released into the extracellular space in considerable amounts during ischemic myocardial injury via an unknown mechanism (15). Based on these observations, we raised the hypothesis that the extracellular S100A1 protein may exert protective effects on myocardial cells. To address this question, the current study focuses on the characterization of the extracellular effects of S100A1 protein on cardiac myocytes and related molecular mechanisms *in vitro*. Indeed, our study identifies the S100A1 protein as a novel cardioprotective factor, because we could

* This work was supported in part by Forschungsförderungsprogramm, Medizinische Fakultät der Universität Heidelberg Grants 93/2002 and 61/2003 (to P. M.), Deutsche Forschungsgemeinschaft Grant 1083/1-1 (to A. R.), and grants from the M. E. Müller Foundation and the Kanton of Basel Stadt (to M. B. and C.-A. S.). The costs of publication of this article were defrayed in part by the payment of page charges. This article must therefore be hereby marked "*advertisement*" in accordance with 18 U.S.C. Section 1734 solely to indicate this fact.

§ These authors contributed equally to this study.

¶ To whom correspondence should be addressed. Tel.: 49-6221-56-1505; Fax: 49-6221-56-4866; E-mail: patrick.most@med.uni-heidelberg.de.

** Supported by the Boehringer Ingelheim Stiftung.

§§ These authors contributed to and supported this study equally.

[1] The abbreviations used are: MAP, mitogen-activated protein; MAPK, MAP kinase; ERK1/2, extracellular signal-regulated kinase 1/2; MEK, MAPK/ERK kinase; $[Ca^{2+}]_e$, extracellular Ca^{2+}; CPZ, chlorpromazine; 2-DOG, 2-deoxyglucose; MDC, monodansylcadaverine; MTT, 3-(4,5-dimethylthiazol-2-yl)-2,5-diphenyltetrazolium bromide; Myr, myristoylated; NVCM, neonatal ventricular cardiomyocyte; PBS, phosphate-buffered saline; PKA, protein kinase A; PKC, protein kinase C; PLC, phospholipase C; RAGE, receptor for advanced glycosylated end products; Rh-S100A1, rhodamine-conjugated recombinant S100A1 protein; SAPK/JNK, stress-activated protein kinase/ c-Jun NH_2-terminal kinase.

demonstrate for the first time that the extracellular S100A1 protein can protect cardiomyocytes from apoptosis based on Ca^{2+}-dependent clathrin-mediated endocytotic uptake resulting in a specific activation of the pro-survival ERK1/2 signaling pathway.

EXPERIMENTAL PROCEDURES

Reagents—Monodansylcadaverine (M-4008), chlorpromazine (C-8138), and verapamil (V-4629) were purchased from Sigma, whereas myristoylated (Myr) protein kinase A (PKA) inhibitor (Myr-PKI; catalog number 476485), calphostin-c (catalog number 208725), U-73122 (catalog number 662035), and PD98095 (catalog number 513000) were obtained from Calbiochem. Myr-FRCRCF was custom-made by Eurogentec (Belgium) as described previously (16, 17). Anti-receptor for advanced glycosylated end products (anti-RAGE) antibody was obtained from Chemicon (catalog number MAB5328).

Expression and Purification of Human Recombinant S100A1 Protein—Expression and purification of the human recombinant S100A1 protein in *Escherichia coli* were performed as described previously (6). After dialysis against PBS (pH 7.4), aliquots of purified S100A1 were stored at −80 °C. Coupling of S100A1 with tetramethyl-rhodamine (Rh-S100A1) was carried out by Eurogentec.

Cell Culture—Isolation of neonatal ventricular cardiomyocytes (NVCMs) was performed as described previously (18). NVCMs were cultured for 3 days either on plastic culture dishes, glass coverslips, or Cell-Locate™ slides (Eppendorf) in Dulbecco's modified Eagle's medium (Biochrom) supplemented with penicillin/streptomycin (100 units/ml), L-glutamine (2 mM), and 0.5% fetal calf serum (FCS Gold; PAA Laboratories GmbH) (standard medium) at 37 °C in a 95% air/5% CO_2 humidified atmosphere. To induce apoptosis, 2-day old cultures were either incubated in glucose-free standard medium or Dulbecco's modified Eagle's medium containing 2-deoxyglucose (3 mM) or H_2O_2 (100 μM), respectively, for an additional 18 h. NVCMs were treated with 1 μM human recombinant S100A1 where indicated.

Indirect Immunofluorescence and Phase Contrast Images—3-day-old NVCMs grown on glass coverslips were incubated with Rh-S100A1 (1 μM) as indicated, washed three times with PBS (pH 7.4), fixed in 4% paraformaldehyde, and permeabilized with 0.2% Triton X-100 in PBS. Following three PBS washes, coverslips were incubated in 0.1% bovine serum albumin for 30 min to block nonspecific sites. Subsequently, cells were labeled with either anti-α-actinin (Sigma; 1/3000), anti-transferrin (Sigma; 1/500), or anti-caveolin-3 (Santa Cruz Biotechnology; 1/500) antibodies. Following incubation of the primary antibody for 1 h in the dark, coverslips were washed four times with PBS, and then the corresponding ALEXA Fluor 488-conjugated secondary antibody (Molecular Probes; 1/800) was added for 1 h. After several washes with PBS, coverslips were mounted in Mowiol. Confocal images were obtained using a 100× oil objective on a Leica TCS SP laser-scanning confocal microscope. Digitized confocal images were processed by Leica software and Adobe Photoshop. For phase contrast images, an inverse microscope (Olympus IX 70) equipped with a SensiCam CCD camera (PCO Imaging) was used. Images were subsequently processed with TILLvisION4.01 software (Tillphotonics).

Trypan Blue Exclusion, Cytochrome c Release, Caspase-3 Activity, and MTT Assay—The fraction of dead cells was determined by counting trypan blue-stained cells on Cell-Locate™ slides. Viable NVCMs were tested for electrical excitability by field stimulation. On each Cell-Locate™ slide, a total number of at least 150 cells were inspected. Cytochrome *c* release and caspase-3 activity were assessed by Quantikine® M Mouse cytochrome *c* immunoassay (R&D Systems, catalog number MCTC0) and Caspase-3 Colorimetric Assay (R&D Systems, catalog number BF3100), respectively, as outlined by the manufacturer's protocol. An MTT assay based on the reduction of tetrazolium salt (MTT) was purchased from Trevigen (4890–25-K) and carried out according to the manufacturer's protocol.

Western Blot and Mitogen-activated Protein Kinase (MAPK) Activity—Western blots using specific antibodies were performed to assess protein levels of phosphorylated/nonphosphorylated MAP kinases p44/42 (ERK1/2; Cell Signaling catalog number 9101/9102), p38 (Cell Signaling catalog number 9211/9212), p54/46 (SAPK/JNK; Cell Signaling catalog number 9251/9252), cardiac actin (Biogene; Ac1–20.4.2) and S100A1 protein (Eurogentec; SA 5632). Cell cultures were rinsed in PBS and scraped off the dish in lysis buffer (PBS, pH 7.4, SDS 2%, and 2 mM EGTA/EDTA) containing a mixture of 1% (v/v) phosphatase inhibitors (Sigma; phosphatase inhibitor mixture I/II) and protease inhibitor (1 tablet/5 ml) (Roche Applied Science; Mini Complete EDTA-free protease inhibitor). To determine Rh-S100A1-uptake, NVCMs were first washed extensively with EGTA/EDTA buffer (PBS, pH 7.4, and 2 mM EGTA/EDTA) and then lysed. Blots were developed with the Avidix chemiluminescence detection system (Tropix, Applied Biosystems, Foster City, CA) and quantified by densitometry.

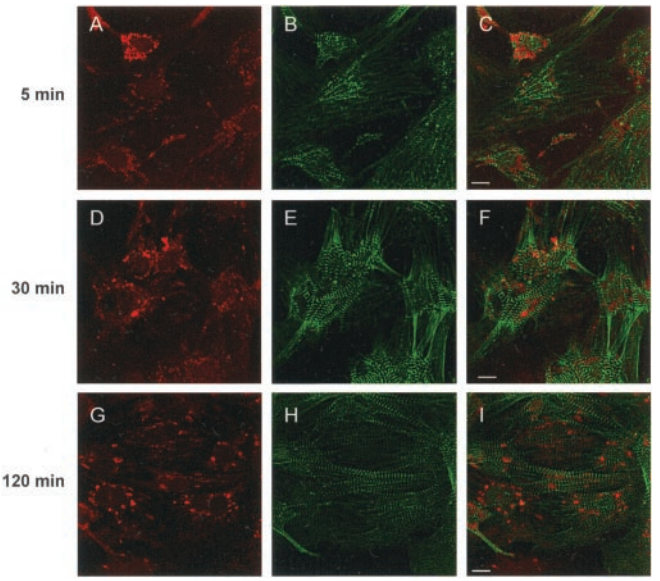

FIG. 1. **Localization of internalized Rh-S100A1 protein in NVCMs.** *A*, *D*, and *G*, in 3-day-old cardiomyocyte cultures, Rh-S100A1 (*red*) is detected intracellularly 5 min after its addition to the culture medium. The overall intracellular distribution of Rh-S100A1 is similar 30 and 120 min after its addition to the culture medium. *B*, *E*, and *H*, to identify cardiomyocytes, the same cultures were immunostained with an anti-α-actinin/Alexa Fluor 488-anti-mouse antibody (*green*), which reveals a distinct striated pattern. *C*, *F*, and *I*, merged images confirming the uptake of Rh-S100A1 by NVCMs. *Bar*, 10 μm.

Statistical Analyses—Data are presented as mean ± S.E. Unpaired Student's *t* test and a two-way repeated analysis of variance (ANOVA) analysis were performed to test for differences between groups. A value of $p < 0.05$ was accepted as statistically significant.

RESULTS

Ca^{2+}-dependent Clathrin-mediated Endocytosis of Extracellular S100A1 Protein in NVCMs—Before studying the effect of extracellularly added S100A1 protein on NVCMs, the purity of human recombinant S100A1 protein was analyzed by SDS-PAGE, and the specificity of S100A1 was confirmed by Western blots probed with an custom-made antibody that specifically recognizes human S100A1 (SA5632) (data not shown) as described recently (6).

Incubation of NVCMs with 1 μM rhodamine-conjugated recombinant S100A1 protein (Rh-S100A1) for 5, 30, and 120 min in the presence of 2 mM extracellular Ca^{2+} ($[Ca^{2+}]_e$) resulted in a vesicular accumulation of the protein in the cytosol as shown by laser-scanned confocal images (Fig. 1). Consistent with a cytosolic distribution of internalized S100A1 protein, images taken at the level of the nucleus revealed nuclear exclusion of Rh-S100A1. Simultaneous indirect immunofluorescence labeling of Rh-S100A1-treated NVCMs with an anti-α-actinin antibody revealed the regular striated Z-line pattern typical of cardiomyocytes. Despite a reported interaction of S100A1 protein with the Z-line component capZ (19), internalized Rh-S100A1 protein seemed not to localize to the Z-lines. This suggests that internalized and endogenous S100A1 proteins are present in distinct cellular compartments, probably serving dual functions in the cardiomyocyte. To further examine the specificity of S100A1 uptake, parallel NVCM cultures were incubated with corresponding concentrations of rhodamine alone. However, in these Rh-treated cells we did not detect any dye uptake (data not shown). In contrast to NVCMs cultured in Ca^{2+}-containing standard medium, a vesicular accumulation of

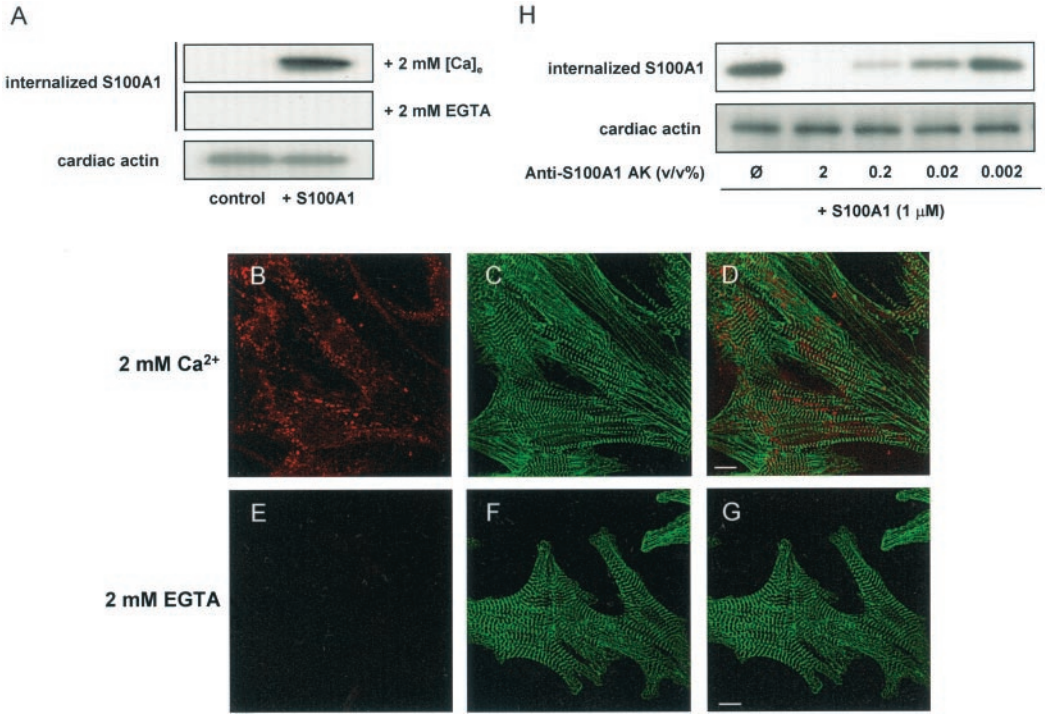

FIG. 2. **Ca^{2+}-dependence of S100A1 internalization.** *A*, Western blot of homogenates of untreated (*control*) and S100A1-treated NVCMs in the presence of 2 mM Ca^{2+} (*upper section*) or 2 mM EGTA (*middle section*) probed with an antibody that is specific for human S100A1. The addition of 2 mM EGTA to the medium prevents cellular uptake of Rh-S100A1. Probing with an antibody that recognizes cardiac actin (*bottom section*) demonstrates that the protein loading in individual lanes was comparable. *B*, fluorescence image showing the cellular uptake of exogenously added Rh-S100A1 (*red*) in the presence of 2 mM $[Ca^{2+}]_e$ after 30 min. *C*, immunostaining with an anti-α-actinin antibody reveals the striated pattern typical for cardiomyocytes. *D*, merged image of Rh-S100A1 and Alexa Fluor 488-α-actinin in the presence of 2 mM $[Ca^{2+}]_e$. *Bar*, 10 μm. *E*, internalization of Rh-S100A1 does not occur in the presence of 2 mM EGTA. *F*, immunostaining of Rh-S100A1-treated NVCMs in the presence of 2 mM EGTA with an anti-α-actinin/Alexa Fluor 488-anti-mouse antibody. *G*, merged image of *panels E* and *F* reveals only the striated pattern typical for cardiomyocytes but without Rh-S100A1 uptake. *Bar*, 10 μm. *H*, Western blot of homogenates prepared from S100A1-treated (1 μM) NVCM cultures that were incubated with different amounts of anti-S100A1 antibody (*Anti-S100A1 AK*) (SA 5632; 2–0.002%, v/v). The uptake of extracellularly added S100A1 is inhibited by SA 5632 in a dose-dependent manner. The band representing human S100A1 is no longer detected if SA 5632 is present in the culture medium at 2% (v/v).

Rh-S100A1 protein was not observed in cells that were kept in Ca^{2+}-free medium containing 2 mM EGTA (Fig. 2, *B–G*). This absence indicates that the uptake of exogenous S100A1 is dependent on Ca^{2+}. Analysis of homogenates from control NVCMs and cells treated with S100A1 in the presence and absence of Ca^{2+} by anti-S100A1 Western blotting further confirmed the Ca^{2+}-dependence of S100A1 internalization (Fig 2*A*). Moreover, if NVCM cultures were incubated for 20 min with anti-S100A1 antibody (SA 5632) prior to the addition of recombinant S100A1, uptake of the S100A1 protein was also inhibited (Fig. 2*H*). As expected for a specific inhibition, the antibody-mediated "clearing" was dose-dependent, and, thus, an unspecific cellular uptake of the protein driven by the rhodamine tag could be excluded. In contrast, despite previous reports that have identified RAGE as a potential S100 protein receptor, intracellular uptake of S100A1 could not be prevented by a 30-min preincubation with an anti-RAGE antibody (10 μg/ml) that recognizes the ligand-binding domain of the receptor (MAB5328; data not shown) (11, 20).

To gain insight into the pathway of S100A1 internalization, Rh-S100A1-treated NVCMs were labeled with an anti-caveolin-3/Alexa Fluor 488-anti-mouse antibody (Fig. 3), which is a marker for the caveolin-mediated uptake (21). Merging the corresponding rhodamine and Alexa Fluor 488 confocal images clearly showed that the caveolin-3 staining pattern is distinct from that of Rh-S100A1 vesicles (Fig. 3*C*). In contrast, immunolabeling of Rh-S100A1-treated NVCMs with an anti-transferrin antibody, which is a marker for the endosomal compartment, revealed that Rh-S100A1 vesicles colocalize with transferrin and are therefore part of the endosomal compartment (Fig. 3, *D–F*) (22, 23). To substantiate that a clathrin-mediated uptake rather than a caveolin-dependent process is involved in S100A1 internalization, we examined the effects of two inhibitors of clathrin-mediated endocytosis, monodansylcadaverine (MDC) and chlorpromazine (CPZ) (24, 25), on the

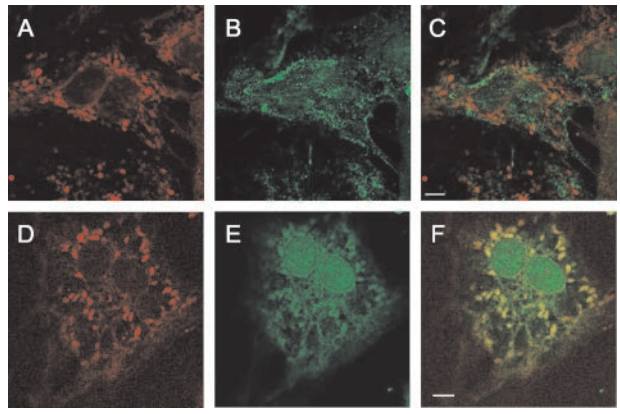

FIG. 3. **Colocalization of internalized Rh-S100A1 with the endosomal compartment.** *A*, vesicular accumulation of Rh-S100A1 in the cytoplasm. *B*, immunostaining of Rh-S100A1-treated NVCMs with an anti-caveolin-3/Alexa Fluor 488-anti-mouse antibody, which outlines the caveolin-mediated pathway. *C*, overlay of *panels A* and *B* shows no colocalization. *D*, vesicular accumulation of Rh-S100A1 in the cytoplasm. *E*, labeling of the endosomal compartment in Rh-S100A1-treated NVCMs with an anti-transferrin/Alexa Fluor 488-anti-mouse antibody. *F*, overlay of *panels E* and *F* reveals colocalization of Rh-S100A1 and transferrin. *Bar*, 5 μm.

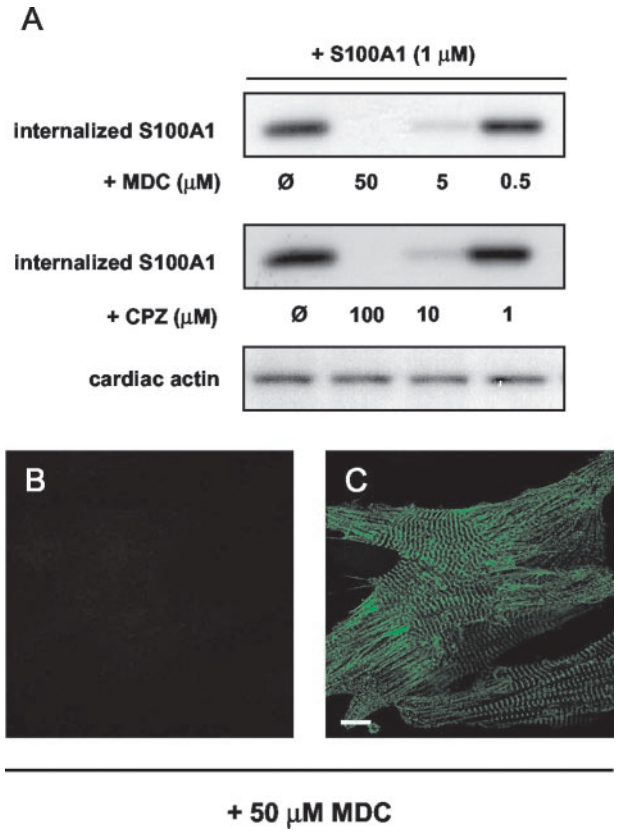

FIG. 4. **Clathrin-mediated endocytosis of S100A1 in NVCMs.** *A*, Western blots of homogenates of S100A1-treated NVCMs incubated in the presence of MDC (*upper section*) and CPZ (*middle section*), respectively. Internalized S100A1 is detected with an anti-human S100A1-specific antibody (SA 5632), whereas an anti-cardiac actin antibody was used to normalize amounts of protein loaded in individual lanes (*bottom section*). Inhibition of S100A1 uptake via the clathrin-mediated pathway by MDC and CPZ is dose-dependent. *B*, fluorescence image of Rh-S100A1-treated (1 μM) NVCMs incubated with standard medium containing 50 μM MDC. Vesicular accumulation of Rh-S100A1 in the cytoplasm is not detected if clathrin-mediated endocytosis is blocked by MDC. *C*, immunolabeling of the same coverslip with an anti-α-actinin/Alexa Fluor 488-anti-mouse antibody confirms the presence of cardiomyocytes. *Bar*, 10 μm.

uptake of S100A1. As illustrated by Western blots of homogenates of cells incubated with S100A1 in the presence of inhibitors that were probed with an anti-human S100A1 antibody (Fig. 4*A*), MDC and CPZ resulted in a dose-dependent inhibition of S100A1 internalization. Consistently, laser-scanned confocal images of NVCMs incubated with S100A1 in the presence of MDC revealed an absence of Rh-S100A1-uptake (Fig. 4*B*).

In conclusion, our data strongly suggest that the extracellular S100A1 protein is internalized and routed for the endosomal compartment of NVCMs via a Ca^{2+}-dependent, clathrin-mediated endocytotic pathway. Because RAGE apparently does not mediate internalization of the extracellular S100A1 protein in NVCMs in our experimental setting, the S100A1 protein may be endocytosed by another, yet to be identified receptor.

Activation of the ERK1/2 Signaling Pathway by Endocytosed S100A1—Because signaling proteins of the MAPK pathways in particular have been linked to the endosomal compartment (for review, see Ref. 25), we next investigated whether endocytotic uptake of the S100A1 protein might affect MAPK activity in NVCMs. For this purpose, Western blots of homogenates were probed with antibodies that specifically recognize either the unphosphorylated or the phosphorylated form of the respective protein. Fig. 5*A* shows that the addition of 1 μM S100A1 to NVCM in the presence of 2 mM $[Ca^{2+}]_e$ resulted in a specific increase of p44/42 (ERK1/2) phosphorylation (3.8-fold; Fig. 5*A*, *upper section*) compared with control cells. Consistently, if S100A1-uptake is prevented by the presence of 2 mM EGTA (see Fig. 2*A*), S100A1-mediated activation of ERK1/2 was absent. In contrast, the extent of phosphorylation of SAPK/JNK (p54/46; Fig. 5*A*, *middle section*) and p38 (Fig. 5*A*, *lower section*) following Ca^{2+}-dependent S100A1 uptake was comparable with that of control cells (Fig. 5*A*). Incubation of NVCMs with S100A1 protein (1 μM) in the range of 1 to 30 min showed a time dependence of ERK1/2 activation (Fig. 5*B*), whereas a 30-min application of increasing concentrations of extracellular S100A1 protein (0.01–10 μM; Fig. 5*C*) resulted in a dose-dependent enhancement of ERK1/2 phosphorylation. Concomitantly, the concentration of endocytosed S100A1 protein increased (Fig. 5, *B* and *C*). Inhibition of S100A1 endocytosis by 50 μM monodansylcadaverine effectively abrogated the S100A1-mediated increase in ERK1/2 phosphorylation (Fig. 6*A*). Furthermore, S100A1-mediated activation of ERK 1/2 could be prevented by preincubation with PD98095 (2–10 μM) (Fig. 6*B*), a specific inhibitor of MEK1 (26, 27).

Because the extracellular neurotrophic effects of S100A4 protein on rat hippocampal neurons depend on phospholipase C (PLC), which has also been linked to the endosomal compartment, we investigated the influence of PLC inhibition by U-73122 (5 μM) on S100A1-mediated ERK1/2 activation (13, 25). As illustrated in Fig. 6*C*, it appears that the inhibition of PLC completely prevented the S100A1-induced enhancement of ERK1/2 phosphorylation. Because receptor-mediated activation of PLC is known to subsequently enhance protein kinase C (PKC) activity, we next tested whether S100A1-mediated enhancement of ERK1/2 activity requires activation of PKC. Interestingly, in the presence of calphostin-c (0.5 μM), a potent inhibitor of PKC (13), S100A1-induced enhancement of ERK1/2 phosphorylation was abrogated (Fig. 6*C*). Because activation of cAMP-dependent protein kinase (PKA) has also been linked to ERK1/2 signaling, we likewise explored the effect of PKA inhibition on S100A1-dependent ERK1/2 activation by a cell-permeable specific PKA inhibitor (28). However, preincubation of NVCMs with the Myr-PKA inhibitor (5 μM) 14-22 amide for 30 min did not affect S100A1-mediated enhancement of ERK1/2 activity (Fig. 6*C*). This finding suggests that the modulation of the ERK1/2 signaling pathway by S100A1 does not involve PKA.

Transsarcolemmal Ca^{2+} influx has been shown to be another modulator of ERK1/2 signaling (28). Because the exogenous addition of the S100A1 protein to immature cardiomyocytes has been shown to increase L-type Ca^{2+}-channel (dihydropyridine receptor) activity and thus Ca^{2+} influx (29), we explored the effect of extracellularly added S100A1 protein on ERK1/2 signaling in response to inhibition of transsarcolemmal Ca^{2+} influx. For this purpose, the dihydropyridine receptor was blocked with verapamil (5 μM), and the sodium-calcium exchanger was blocked with a cell-permeable specific sodium-calcium exchanger inhibitor, Myr-FRCRCF (10 μM), In both cases, the inhibitors slightly reduced the extent of ERK1/2 phosphorylation in control cells as well as in S100A1-treated cardiomyocytes but did not perturb the S100A1-uptake and S100A1-mediated activation of ERK1/2 phosphorylation (S100A1 *versus* control, 3.2 ± 0.4-fold, $n = 3$, $p < 0.01$; S100A1 *versus* control (verapamil/Myr-FRCRCF), 2.8 ± 0.2-fold, $n = 3$, $p < 0.01$) (Fig. 6*D*).

Taken together, our results strongly support the notion that the endocytosed S100A1 protein specifically increases ERK1/2 activity via the PLC-PKC-MEK1 pathway. In contrast, PKA and transsarcolemmal Ca^{2+} influx did not appear to be in-

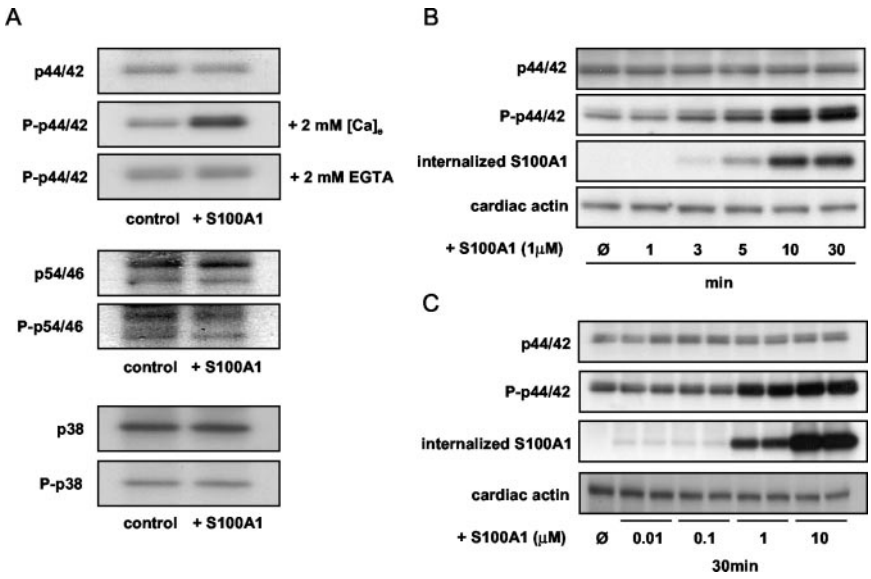

FIG. 5. **Extracellular S100A1 addition specifically increases levels of phosphorylated ERK1/2 (P-p44/42).** *A*, the effects of extracellularly added S100A1 (1 μM) on the levels of unphosphorylated and phosphorylated p44/42 (ERK1/2; *top sections*), p55/46 (SAPK/JNK; *middle sections*), and p38 (*bottom sections*) are shown by Western blots of cell extracts from untreated (*control*) and S100A1-treated cardiomyocytes (*+S100A1*; 1 μM) probed with specific antibodies. *Top three sections*, Ca^{2+}-mediated uptake of S100A1 leads to a 3.8 ± 0.3-fold increase in p44/42 phosphorylation (*P-p44/42*; *center*) compared with control ($p < 0.01$, $n = 3$), whereas the levels of unphosphorylated p44/42 (*upper*) remain constant. Inhibition of S100A1-uptake by 2 mM extracellular EGTA (*lower*) prevents ERK1/2 activation. *Middle* and *bottom sections*, p54/46 and p38 phosphorylation states are not affected by endocytosed S100A1. *B*, time-dependence of S100A1-induced activation of p44/42 phosphorylation (*P-p44/42*). The increase in p44/42 phosphorylation coincides with an increased level of internalized S100A1 over time. Maximal S100A1-uptake and phosphorylated p44/42 levels are reached after 10 min. *C*, dose-dependent activation of ERK1/2 phosphorylation. NVCMs were incubated with increasing amounts of S100A1 (0.01–10 μM) for 30 min. A significant ($p < 0.01$) increase of phosphorylated p44/42 is detected at 1 and 10 μM S100A1 stimulation.

volved in the S100A1-mediated activation of ERK1/2.

S100A1 Inhibits NVCM Apoptosis via ERK1/2 Signaling—Previous studies that have demonstrated that ERK1/2 activation is associated with protection from apoptosis in cardiomyocytes (26, 30–33), prompted us to examine whether S100A1-induced ERK1/2 signaling may exert cardioprotective effects on cardiomyocytes. To assess whether the addition of S100A1 provides protection from apoptotic stimuli, NVCMs were incubated in 2-deoxyglucose (2-DOG) containing glucose-free medium for 18 h as described previously (26) and in 2-DOG containing the MEK1 inhibitor PD98095. Fig. 7 shows corresponding phase contrast images of NVCMs cultured in standard medium in comparison to cells cultured in 2-DOG. The addition of S100A1 to NVCMs cultured in standard medium did not significantly alter cell morphology (Fig. 7, *A* and *B*). Apoptosis is induced when NVCMs were cultured in 2-DOG rather than standard medium (Fig. 7*C*), and the cells display a rounded morphology. In the presence of S100A1 (Fig. 7*D*), the rounding up of 2-DOG was prevented, and the cell morphology is similar to that of untreated cells cultured in standard medium (Fig. 7*A*). The S100A1-induced protection from apoptosis was abolished in the presence of the MEK1 inhibitor PD98095 (Fig. 7*F*).

The viability of NVCMs was assessed by trypan blue exclusion and electrical field stimulation (Fig. 7*G*). The addition of 1 μM S100A1 protein did not affect the viability of cells under standard culture conditions (S100A1-treated 117 ± 8, *versus* untreated 119 ± 8, each $n = 5$ cell locates; p values were not significant). However, compared with untreated NVCMs (100%), only ~30% of cells cultured in 2-DOG were viable and able to contract. When the cells were treated with S100A1 (1 μM), the survival rate of 2-DOG-induced apoptotic cells was ~2-fold higher. Consistent with the morphological data, S100A1-mediated rescue from apoptosis was effectively abolished by the presence of the MEK1 inhibitor PD98095 (10 μM).

As additional indicators of apoptosis, mitochondrial cytochrome *c* release, caspase-3, and mitochondrial dehydrogenase activity were quantified under different culture conditions (Fig. 7, *H–J*). If S100A1 was added to cells cultured in 2-DOG medium, the cytochrome *c* release and caspase-3 activity was reduced by ~2.5- and ~1.8-fold, respectively (Fig. 7, *H* and *I*). Again, the S100A1-mediated protection from apoptosis was effectively prevented by the addition of 10 μM PD98095. The presence of the inhibitor also blocked a nearly ~1.3-fold higher preservation of mitochondrial dehydrogenase activity in S100A1-treated cells compared with untreated NVCMs (Fig. 7*J*). In line with these results, the pretreatment of cultured cardiomyocytes with S100A1 similarly inhibited oxidative stress-induced apoptosis by H_2O_2 (100 μM) in our experimental setting (data not shown). In summary, these results demonstrate that the addition of the S100A1 protein to cultured neonatal ventricular cardiomyocytes protects them via the activation of ERK1/2 signaling from apoptotic stimuli.

DISCUSSION

To date, the multigene family of Ca^{2+}-binding proteins of the EF-hand type known as S100 proteins has grown to 21 members that are differentially expressed in a large number of cell types. Individual S100 proteins are viewed as cell-specific proteins, which are implicated in the Ca^{2+}-dependent regulation of a variety of activities in the cell (3). Recent evidence indicates that S100 proteins, once secreted or released into the extracellular space, may also exert specific effects on their target cells. For instance, extracellular S100A8 and S100A9 secreted by a novel tubulin-dependent pathway have been ascribed important functions in the regulation of inflammatory processes (9). In addition, secreted S100B, S100A4, and S100A12 have been shown to exert a neurotrophic effect on neurons (11, 13, 14). In the case of S100B, the trophic effects on neurite outgrowth were accompanied by an increased expression of the anti-apoptotic protein Bcl-2 (11). Because S100A1 is also released into the extracellular space following ischemic

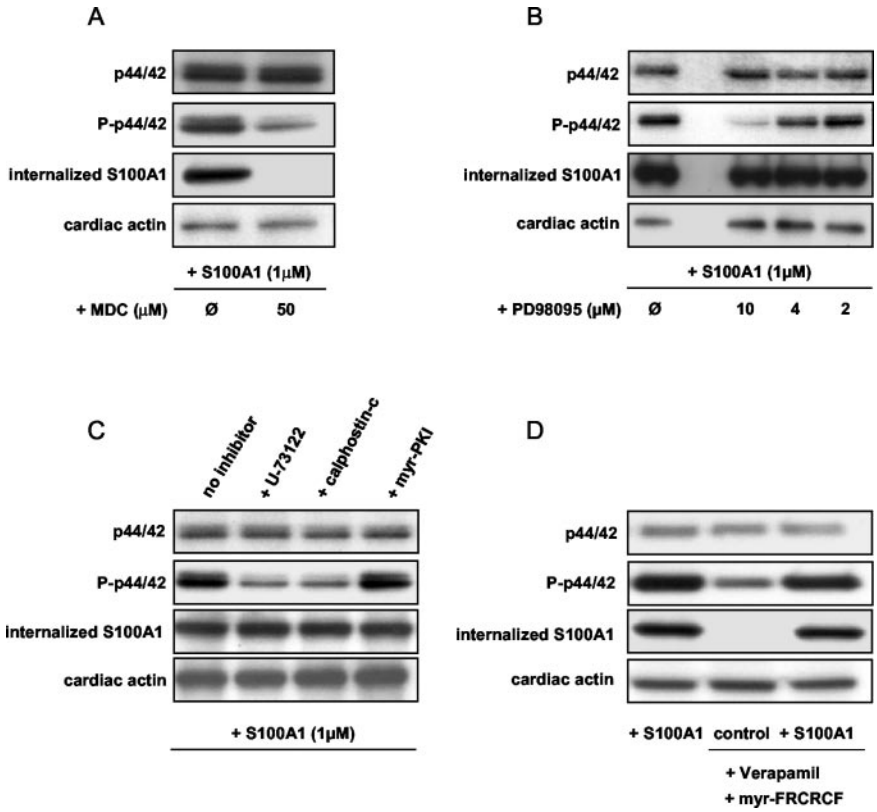

FIG. 6. **Effects of S100A1 on the signaling pathway upstream of ERK1/2.** *A*, Western blot of extracts from cells treated with S100A1 in the presence of 50 μM MDC and probed with specific antibodies; S100A1 uptake as well as S100A1-mediated increase of ERK1/2 phosphorylation (*P-p44/42*) is inhibited. *B*, addition of increasing amounts of MEK1 inhibitor PD98095 (2, 4, and 10 μM) to S100A1-stimulated NVCMs. Western blots of homogenates show that S100A1-uptake is not affected by PD98095, whereas the levels of phosphorylated ERK1/2 (*P-p44/42*) are reduced in a dose-dependent manner. *C*, effects of PLC, PKC, and PKA inhibition on S100A1-mediated activation of ERK1/2 phosphorylation (*P-p44/42*). In the presence of PLC inhibitor U-73122, levels of phosphorylated p44/42 are significantly reduced. A similar effect is observed by inhibition of PKC with calphostin-c. In contrast, inhibition of PKA by the Myr-PKA inhibitor has no effect on the levels of phosphorylated p44/42. Probing the Western blot with an anti-S100A1 antibody shows that S100A1 endocytosis (internalized S100A1) is not influenced by the inhibitors of PLC, PKC, and PKA. *D*, effects of transsarcolemmal Ca^{2+} influx on ERK1/2 phosphorylation. Simultaneous inhibition of L-type Ca^{2+}-channel (5 μM verapamil) and a sodium-calcium exchanger inhibitor (Myr-FRCRCF; 10 μM) leads to a reduction of phosphorylated p44/42 (*P-p44/42*) levels in untreated (*control*) cells and S100A1-treated cells by ~40%. Both S100A1 uptake (*internalized S100A1*) and S100A1-mediated activation of ERK1/2 are not significantly perturbed. Equal protein loading in individual lanes was confirmed by comparable levels of cardiac actin.

myocardial injury (15), we undertook this study addressing the question of whether extracellular S100A1 may exert protective effects on cardiac cells.

Our data provide, for the first time, evidence that the extracellular addition of the S100A1 protein can protect neonatal ventricular cardiomyocytes from apoptosis *in vitro* via specific activation of the ERK1/2 signaling pathway. By coupling the human recombinant S100A1 protein with rhodamine, we were able to trace the uptake of S100A1 into the cytosolic compartment of cultured NVCMs. Indirect immunofluorescence staining and uptake experiments under different culture conditions revealed that the S100A1 protein is internalized via a Ca^{2+}-dependent clathrin-mediated endocytotic pathway. Interestingly, our results suggest that cell surface RAGE, which has been reported to interact with S100B (11, 20), does not seem to be involved in the endocytosis of S100A1 in NVCMs. Therefore, another cell surface receptor is likely to be responsible for S100A1 uptake in NVCMs. Recently, internalization of the S100A1 protein into embryonic murine cardiomyocytes has been shown to be associated with a decrease in membrane capacitance (29). With regard to the current study, this decrease in membrane capacitance is likely to reflect endocytotic vesicles forming at the plasma membrane, which then pinch off as clathrin-coated vesicles and eventually fuse with the endosomal compartment.

A growing body of evidence indicates that several signaling proteins involved in receptor tyrosine kinase and G-protein coupled receptor signal transduction, *e.g.* PLC, Ras, Raf, MEK1, and ERK1/2, are located in endosomes from where they transduce signals to the cytosol and nucleus (25). In hippocampal neurons, it has been shown that the extracellular addition of the S100A4 protein activates the ERK1/2 signaling pathway (13). Correspondingly, our data obtained from Western blots probed with antibodies that specifically recognize unphosphorylated or phosphorylated forms of ERK1/2, together with the Western blot data obtained when known upstream constituents of the MAPK signaling pathway were inhibited (Fig. 8), demonstrate that the internalized S100A1 protein specifically activates ERK1/2 in cardiomyocytes both in a time- and a dose-dependent manner. Thus, internalization of the S100A1 protein represents an important prerequisite for the activation of ERK1/2, because prevention of S100A1 endocytosis, both in Ca^{2+}-free medium and in the presence of inhibitors of clathrin-mediated endocytosis, resulted in a lack of enhanced ERK1/2 phosphorylation. In contrast, kinases involved in other signaling pathways, such as p38 and SAPK/JNK (p54/46), are not affected.

By using several specific inhibitors of intracellular signal transduction constituents (see Fig. 8), we could elucidate that S100A1-mediated activation of ERK1/2 signaling involves activation of PLC and PKC, which have been closely linked to the endosomal compartment (25). A stimulation of ERK1/2 activation by PKC has been reported previously (34). Based on our collective findings, we have developed a model of how S100A1 participates in the ERK1/2 signaling cascade (Fig. 8). As de-

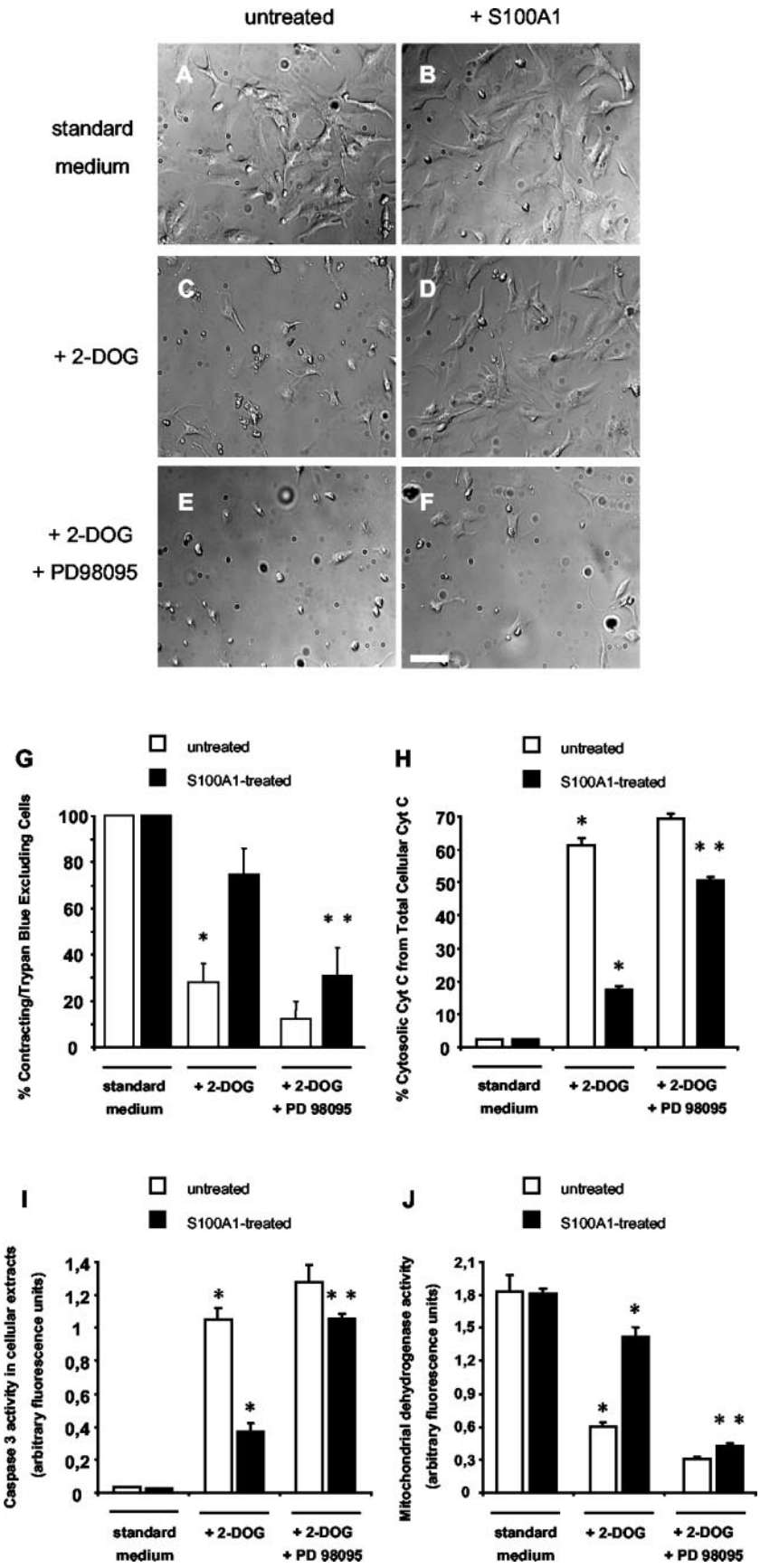

FIG. 7. **Antiapoptotic effect of S100A1 protein on NVCMs.** *A–F*, phase contrast images of NVCMs under different culture conditions. *A*, untreated cells in standard culture medium (containing glucose) (*control*). *B*, addition of S100A1 (1 μM) to NVCMs in standard medium does not significantly alter their morphology. *C*, NVCMs cultured for 18 h in medium containing the apoptosis-inducing 2-DOG (3 mM) without S100A1 display a rounded morphology. *D*, if S100A1 is added to the cells, cells cultured in 2-DOG extend cellular processes and assume a morphology similar to that of control cells (*panel A*). *E*, untreated cells cultured as in *panel C* but in the presence of the MEK1 inhibitor PD98095 do not spread. *F*, in the presence of PD98095, 2-DOG-induced apoptosis is not overcome by the addition of S100A1. *Bar*, 50 μm. *G*, anti-apoptotic effect of S100A1 involves the ERK1/2 pathway. Compared with control NVCMs (*standard medium*, no S100A1; 100%), only 28 ± 3.6% of cells ($n = 5$) cultured in 2-DOG were viable and able to contract. When cells were treated with S100A1 (1 μM), the survival rate of 2-DOG-induced apoptotic cells is ~2-fold higher (79 ± 5.6%; *, $p < 0.01$) compared with control cells. The addition of 10 μM PD98095 abolishes the S100A1-induced rescue (30 ± 5.8% survival, $n = 5$; **, $p < 0.01$). *H*, S100A1 treatment reduces apoptosis-related mitochondrial cytochrome *c* release by ~2.5-fold (S100A1 17 ± 1.1% *versus* untreated 61 ± 2.3%, $n = 5$; *, $p < 0.01$; data are expressed as the percentage of cytosolic cytochrome *c* from total cytochrome *c* (*Cyt c*); total cytochrome *c* was estimated at ~230 ng per 10^6 cells). This reduction is blocked by 10 μM PD98095 (S100A1-treated 17 ± 1.1% *versus* S100A1-treated/PD98095 50.4 ± 2.1%, $n = 5$; **, $p < 0.01$). *I*, apoptosis-related caspase-3 activity is reduced ~1.8-fold by S100A1 treatment (S100A1-treated 0.37 ± 0.08 *versus* untreated 1.05 ± 0.1, $n = 5$; *, $p < 0.01$). The anti-apoptotic effect of S100A1 treatment is effectively inhibited by 10 μM PD98095 (S100A1-treated 0.37 ± 0.08 *versus* S100A1-treated/PD98095 1.05 ± 0.046, $n = 5$; **, $p < 0.01$). *J*, in comparison to untreated NCVM, S100A1 treatment prevents the 2-DOG-mediated decrease in mitochondrial dehydrogenase activity (S100A1-treated 1.4 ± 0.2 *versus* untreated 0.6 ± 0.1, $n = 5$; *, $p < 0.01$). This anti-apoptotic effect is inhibited by 10 μM PD98095 (S100A1-treated 1.4 ± 0.2 *versus* S100A1-treated/PD98095 0.4 ± 0.1, $n = 5$; **, $p < 0.01$).

picted by the model, our data also provide evidence that sarcolemmal Ca^{2+} influx mediated by the L-type channel does not participate in the S100A1-mediated enhancement of ERK1/2 phosphorylation. These findings are in contrast to work by Gomez *et al.*, which shows that glucagon-like peptide 1 (GPL-1)-mediated activation of ERK1/2 requires Ca^{2+} influx through L-type channel in a mouse pancreatic β-cell line (28). Moreover, in their experimental system, inhibiting PKA activity dimin-

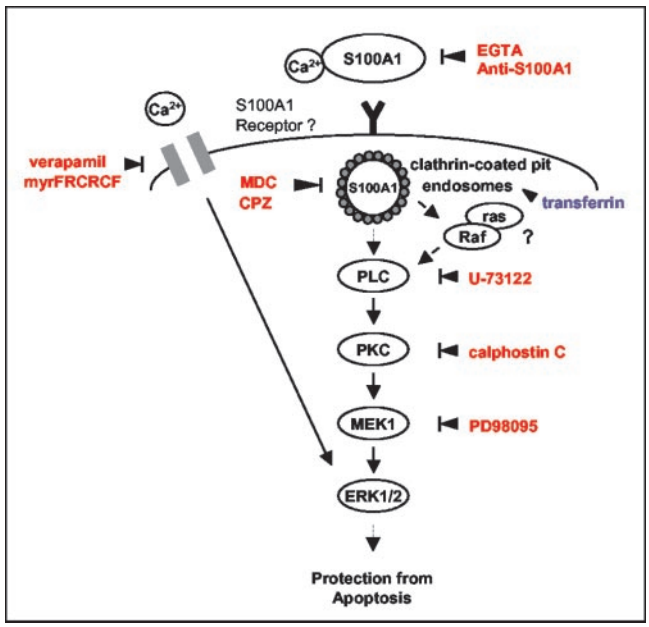

FIG. 8. **Model of S100A1 involvement in ERK1/2 signaling.** The model suggests endocytosis of extracellular S100A1 by NVCMs via an unknown receptor. Inhibitors of the S100A1-mediated pathway are shown in *red*, whereas markers are given in *blue*.

ished glucagon-like peptide 1-mediated ERK1/2 activation, whereas inhibition of PKA showed no significant effect on the S100A1-mediated ERK1/2 activation in NVCMs. In addition, an unchanged phosphorylation state at serine16 in phospholamban in NVCMs after the addition of S100A1 revealed no evidence for enhanced PKA activity in our experimental setting (data not shown). From these differences we conclude that S100A1-mediated ERK1/2 activation follows a different signaling pathway than glucagon-like peptide 1. Taken together, our results strongly support the notion that internalized S100A1 protein is routed to the endosomal compartment where it specifically activates the ERK1/2 signaling pathway.

Because activation of the ERK1/2 signaling pathway by different means has been reported to protect cardiomyocytes from apoptosis (26, 30, 32, 33, 35), we examined whether S100A1 treatment had a similar effect on the viability of neonatal cardiomyocytes in response to the apoptosis-inducing agent 2-deoxyglucose. Indeed, our data show that the S100A1 protein dramatically enhances the survival of cardiomyocytes in response to 2-DOG. S100A1-treated cells at the same time display a reduced release of mitochondrial cytochrome *c*, a diminished caspase-3 activity, and maintain their mitochondrial dehydrogenase activity. In accordance, the pretreatment of cultured cardiomyocytes with S100A1 similarly inhibited oxidative stress-induced apoptosis by H_2O_2 (100 μM) in our experimental setting (data not shown), further corroborating the cytoprotective effect of the S100A1 protein. Consistent with the S100A1 signaling pathway outlined in Fig. 8, these pro-survival parameters are effectively blocked if MEK1 is inhibited by PD98095. Taken together, the data of our study provide convincing evidence that the antiapoptotic effect of S100A1 uptake *in vitro* is brought about by enhanced ERK1/2 signaling. The results of the present study provide the basis for the working model shown in Fig. 8, which illustrates the downstream signaling pathways involved in the antiapoptotic actions of extracellular S100A1 on cardiomyocytes. In conclusion, our study identifies the extracellular S100A1 protein as a novel antiapoptotic factor that enhances survival of neonatal cardiomyocytes *in vitro* via activation of the PLC-PKC-MAP kinase kinase1-ERK1/2 pathway.

The mechanism by which a considerable amount of S100A1 is released into the extracellular space during ischemic myocardial injury is yet unknown. Because other S100 proteins are secreted either by a Ca^{2+}- or a tubulin-dependent pathway, one might consider a similar mechanism for myocardial S100A1 release. Based on these considerations, we hypothesize that, *in vivo*, S100A1 extrusion from myocardial cells under pathological conditions might promote the survival of the surrounding myocardium. Because S100A1 protein levels are reduced in heart failure (36) and S100A1 gene deletion resulted in progressive deterioration of cardiac function *in vivo* (8), S100A1 protein deficiency may not only result in impaired contractility of the failing heart but may also contribute to an enhanced susceptibility of injured or failing cardiomyocytes to apoptosis. Undoubtedly, elucidating the detailed molecular mechanism of myocardial S100A1 release is now imminent, as are studies that provide insight into the pathophysiological relevance of the cardioprotective effect of the S100A1 protein on cardiac cells *in vivo*.

REFERENCES

1. Zimmer, D. B., Cornwall, E. H., Landar, A., and Song, W. (1995) *Brain Res. Bull.* **37,** 417–429
2. Heizmann, C. W., and Cox, J. A. (1998) *Biometals* **11,** 383–397
3. Donato, R. (2003) *Microsc. Res. Tech.* **60,** 540–551
4. Most, P., Bernotat, J., Ehlermann, P., Pleger, S. T., Borries, M., Niroomand, F., Pieske, B., Janssen, P. M., Eschenhagen, T., Karczewski, P., Smith, G. L., Koch, W. J., Katus, H. A., and Remppis, A. (2001) *Proc. Natl. Acad. Sci. U. S. A.* **98,** 13889–13894
5. Most, P., Remppis, A., Pleger, S. T., Löffler, E., Ehlermann, P., Bernotat, J., Kleuss, C., Heierhorst, J., Ruiz, P., Witt, H., Karczewski, P., Mao, L., Rockman, H. A., Duncan, S. J., Katus, H. A., and Koch, W. J. (2003) *J. Biol. Chem.* **278,** 33809–33817
6. Most, P., Remppis, A., Weber, C., Bernotat, J., Ehlermann, P., Pleger, S. T., Kirsch, W., Weber, M., Uttenweiler, D., Smith, G. L., Katus, H. A., and Fink, R. H. (2003) *J. Biol. Chem.* **278,** 26356–26364
7. Remppis, A., Most, P., Löffler, E., Ehlermann, P., Bernotat, J., Pleger, S. T., Börries, M., Repper, M., Fischer, J., Koch, W. J., Smith, G. L., and Katus, H. A. (2002) *Basic Res. Cardiol.* **97,** I56–I62
8. Du, X. J., Cole, T. J., Tenis, N., Gao, X. M., Kontgen, F., Kemp, B. E., and Heierhorst, J. (2002) *Mol. Cell. Biol.* **22,** 2821–2829
9. Rammes, A., Roth, J., Goebeler, M., Klempt, M., Hartmann, M., and Sorg, C. (1997) *J. Biol. Chem.* **272,** 9496–9502
10. Davey, G. E., Murmann, P., and Heizmann, C. W. (2001) *J. Biol. Chem.* **276,** 30819–30826
11. Huttunen, H. J., Kuja-Panula, J., Sorci, G., Agneletti, A. L., Donato, R., and Rauvala, H. (2000) *J. Biol. Chem.* **275,** 40096–40105
12. Alexanian, A. R., and Bamburg, J. R. (1999) *FASEB J.* **13,** 1611–1620
13. Novitskaya, V., Grigorian, M., Kriajevska, M., Tarabykina, S., Bronstein, I., Berezin, V., Bock, E., and Lukanidin, E. (2000) *J. Biol. Chem.* **275,** 41278–41286
14. Mikkelsen, S. E., Novitskaya, V., Kriajevska, M., Berezin, V., Bock, E., Norrild, B., and Lukanidin, E. (2001) *J. Neurochem.* **79,** 767–776
15. Kiewitz, R., Acklin, C., Minder, E., Huber, P. R., Schafer, B. W., and Heizmann, C. W. (2000) *Biochem. Biophys. Res. Commun.* **274,** 865–871
16. Convery, M. K., Levi, A. J., Khananshvili, D., and Hancox, J. C. (1998) *Pfluegers Arch. Eur. J. Physiol.* **436,** 581–590
17. Hobai, I. A., Khananshvili, D., and Levi, A. J. (1997) *Pfluegers Arch. Eur. J. Physiol.* **433,** 455–463
18. Pinson, A. (1990) in *Cell Culture Techniques in Heart and Vessel* (Piper H. M., ed) pp. 20–35, Springer-Verlag, Berlin-Heidelberg-New York
19. Bianchi, R., Garbuglia, M., Verzini, M., Giambanco, I., Ivanenkov, V. V., Dimlich, R. V., Jamieson, G. A., Jr., and Donato, R. (1996) *Biochim. Biophys. Acta* **1313,** 258–267
20. Hofmann, M. A., Drury, S., Fu, C., Qu, W., Taguchi, A., Lu, Y., Avila, C., Kambham, N., Bierhaus, A., Nawroth, P., Neurath, M. F., Slattery, T., Beach, D., McClary, J., Nagashima, M., Morser, J., Stern, D., and Schmidt, A. M. (1999) *Cell* **97,** 889–901
21. Conner, S. D., and Schmid, S. L. (2003) *Nature* **422,** 37–44
22. Rizzo, M. A., Shome, K., Watkins, S. C., and Romero, G. (2000) *J. Biol. Chem.* **275,** 23911–23918
23. Pol, A., Calvo, M., and Enrich, C. (1998) *FEBS Lett.* **441,** 34–38
24. Howe, C. L., Valletta, J. S., Rusnak, A. S., and Mobley, W. C. (2001) *Neuron* **32,** 801–814
25. Sorkin, A., and Von Zastrow, M. (2002) *Nat. Rev. Mol. Cell Biol.* **3,** 600–614
26. Bueno, O. F., De Windt, L. J., Tymitz, K. M., Witt, S. A., Kimball, T. R., Klevitsky, R., Hewett, T. E., Jones, S. P., Lefer, D. J., Peng, C. F., Kitsis, R. N., and Molkentin, J. D. (2000) *EMBO J.* **19,** 6341–6350
27. Davies, S. P., Reddy, H., Caivano, M., and Cohen, P. (2000) *Biochem. J.* **351,** 95–105
28. Gomez, E., Pritchard, C., and Herbert, T. P. (2002) *J. Biol. Chem.* **277,** 48146–48151

29. Reppel, M., Remppis, A., Sasse, P., Roell, W., Most, P., Hescheler, J., Katus, H. A., and Fleischmann, B. K. (2002) *Eur. Heart J.* **23,** (suppl.) 41 (Abstr. P363)
30. Aikawa, R., Komuro, I., Yamazaki, T., Zou, Y., Kudoh, S., Tanaka, M., Shiojima, I., Hiroi, Y., and Yazaki, Y. (1997) *J. Clin. Invest.* **100,** 1813–1821
31. De Windt, L. J., Lim, H. W., Haq, S., Force, T., and Molkentin, J. D. (2000) *J. Biol. Chem.* **275,** 13571–13579
32. Mehrhof, F. B., Muller, F. U., Bergmann, M. W., Li, P., Wang, Y., Schmitz, W., Dietz, R., and von Harsdorf, R. (2001) *Circulation* **104,** 2088–2094
33. Parrizas, M., Saltiel, A. R., and LeRoith, D. (1997) *J. Biol. Chem.* **272,** 154–161
34. Braz, J. C., Bueno, O. F., De Windt, L. J., and Molkentin, J. D. (2002) *J. Cell Biol.* **156,** 905–919
35. Sheng, Z., Knowlton, K., Chen, J., Hoshijima, M., Brown, J. H., and Chien, K. R. (1997) *J. Biol. Chem.* **272,** 5783–5791
36. Remppis, A., Greten, T., Schafer, B. W., Hunziker, P., Erne, P., Katus, H. A., and Heizmann, C. W. (1996) *Biochim. Biophys. Acta* **1313,** 253–257